

Supplementary Information

Poly(butylene adipate-co-terephthalate) with Synergistically Enhanced Mechanical, Moisture/Oxygen Barrier, and Degradation Performance via Embedding Immobilized Enzyme

Jing Yuan¹, Shitong Cui¹, Zixun Xu¹, Jun Xu¹, Jiaxin Shi^{1}, Jun Ge^{1*} and Baohua Guo^{1*}*

¹Department of Chemical Engineering, Tsinghua University, Beijing 100084, China

*Jiaxin Shi: shijx13@tsinghua.org.cn

*Jun Ge: junge@tsinghua.edu.cn

*Baohua Guo: bhguo@mail.tsinghua.edu.cn

Table S1. Thermal properties of PBAT and PBAT/IE calculated by DSC.

Samples	T_g (°C)	T_m (°C)	T_c (°C)	ΔH_m (J/g)
PBAT45	-31.3	110.1	47.2	12.9
PBAT55	-25.2	146.1	108.5	13.4
PBAT55/IE (1wt%)	-25.7	145.9	107.2	13.3
PBAT55/IE (2wt%)	-26.4	146.1	109.2	12.9
PBAT55/IE (3wt%)	-26.1	146.0	107.9	12.9
PBAT60	-20.7	158.8	128.4	14.1
PBAT60/IE (1wt%)	-20.5	158.9	127.9	13.9
PBAT60/IE (2wt%)	-19.7	159.1	127.5	12.8
PBAT60/IE (3wt%)	-20.2	158.8	127.9	13.6

Table S2. Mechanical properties of PBAT and PBAT/IE.

Samples	Tensile Strength (MPa)	Tensile Strain (%)	Yield Strength (MPa)	Young's Modulus (MPa)
PBAT45	21.4	1600	3.2	31.2
PBAT55	24.6	1040	7.7	78.1
PBAT55/IE (1wt%)	20.2	860	7.5	84.5
PBAT55/IE (2wt%)	22.4	910	6.6	77.0
PBAT55/IE (3wt%)	17.3	820	5.1	76.5
PBAT60	22.1	800	9.5	116.4
PBAT60/IE (1wt%)	22.2	790	11.6	123.5
PBAT60/IE (2wt%)	23.8	890	6.1	105.1
PBAT60/IE (3wt%)	19.0	780	6.3	109.4

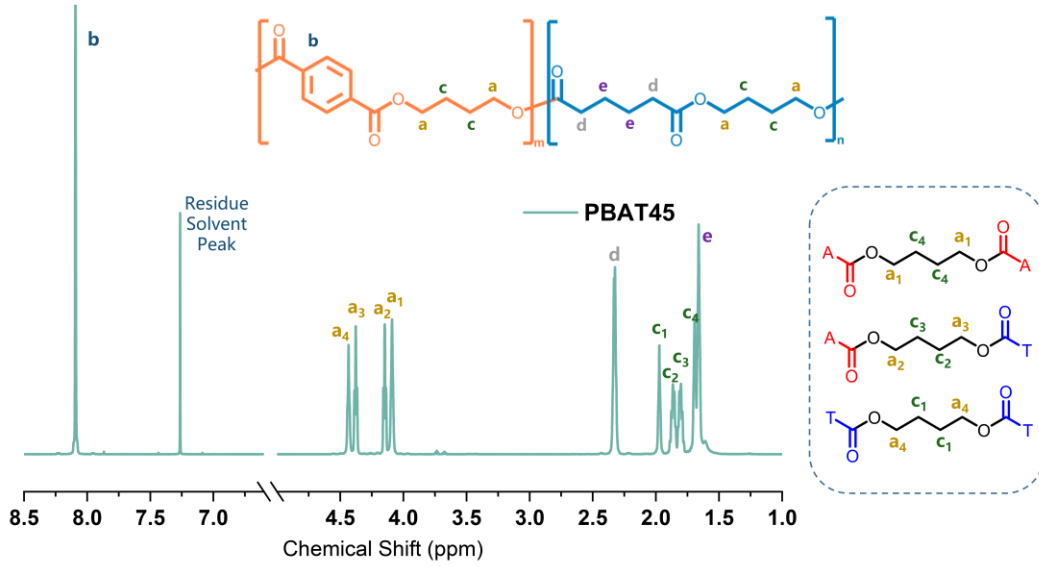


Figure S1. ¹H NMR spectra of PBAT45.

The molar percentages of butylene terephthalate (BT) and butylene adipate (BA) units of PBAT, denoted as n_{BT} and n_{BA} , were determined from the ¹H NMR spectra according to **Equations S1** and **S2**. The average sequence lengths of BT unit (L_{BT}) and BA unit (L_{BA}) were further estimated using **Equations S3** and **S4**.

$$n_{BT} = \frac{I_b}{I_b + I_d} \quad (\text{S1})$$

$$n_{BA} = \frac{I_d}{I_b + I_d} \quad (\text{S2})$$

$$L_{BT} = \frac{I_{a3} + I_{a4}}{I_{a3}} \quad (\text{S3})$$

$$L_{BA} = \frac{I_{a1} + I_{a2}}{I_{a2}} \quad (\text{S4})$$

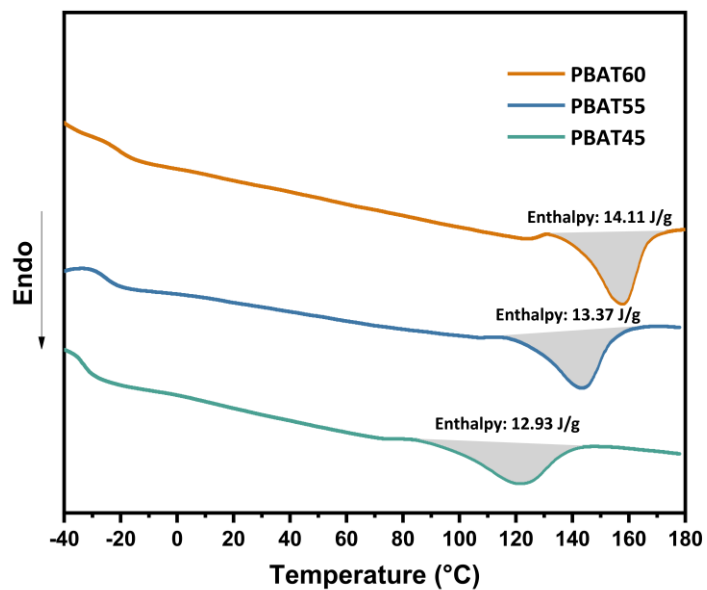


Figure S2. DSC second heating curves and melting enthalpy integration of PBAT45, PBAT55, and PBAT60.

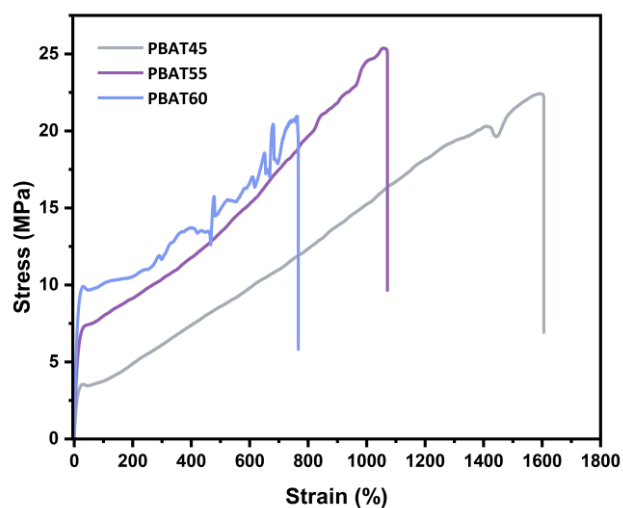


Figure S3. Tensile stress–strain curves of PBAT45, PBAT55, and PBAT60.

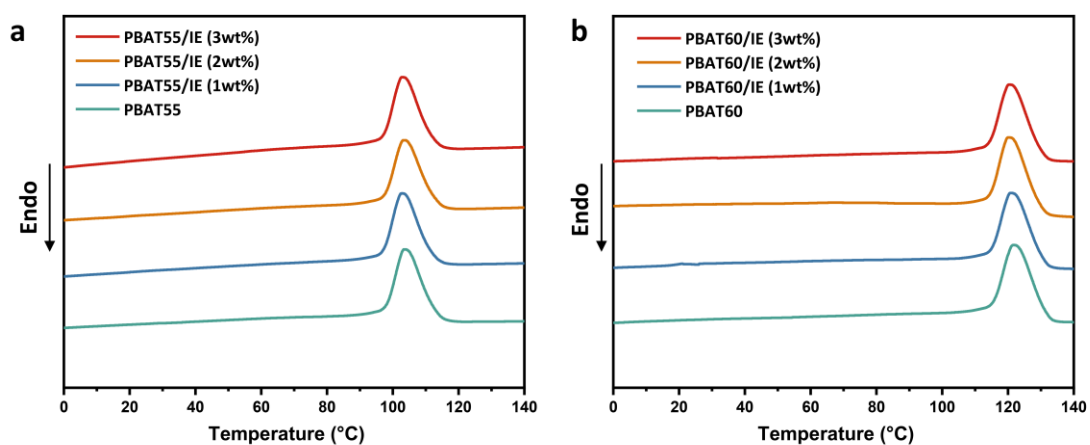


Figure S4. Differential scanning calorimetry (DSC) curves of PBAT55 (a) and PBAT60 (b) with immobilized enzyme nanoparticles at different loadings during first cooling.

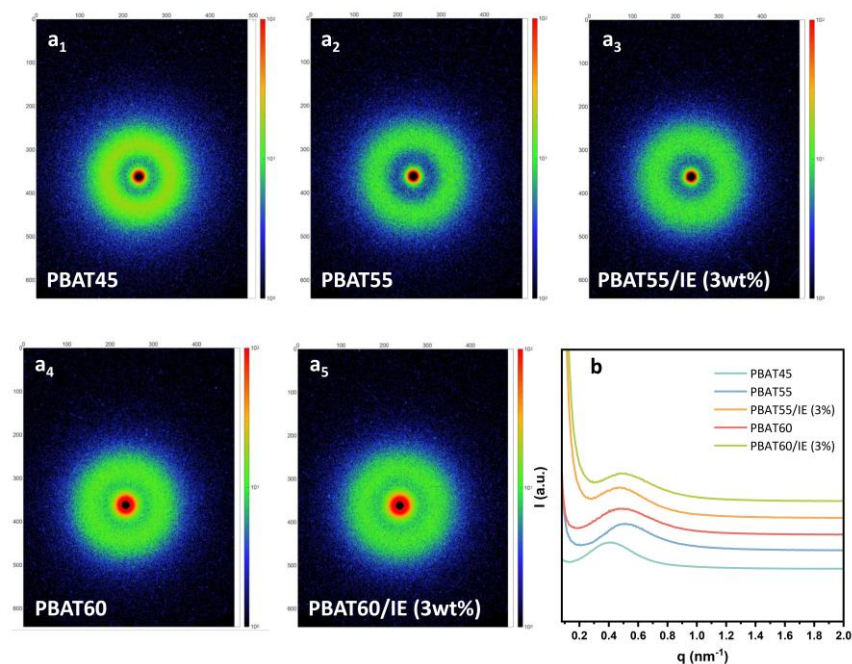


Figure S5. Representative 2D-SAXS patterns and 1D-SAXS curves of PBAT and PBAT with 3wt% immobilized enzyme.

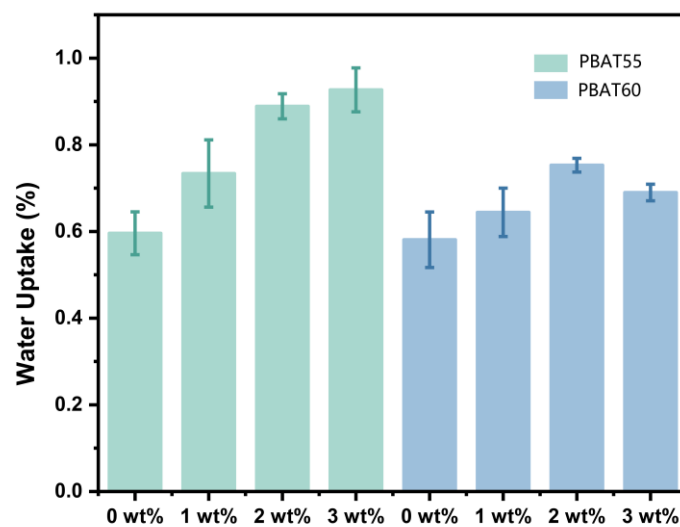


Figure S6. Static water uptake of PBAT with different addition of immobilized enzyme nanoparticles.

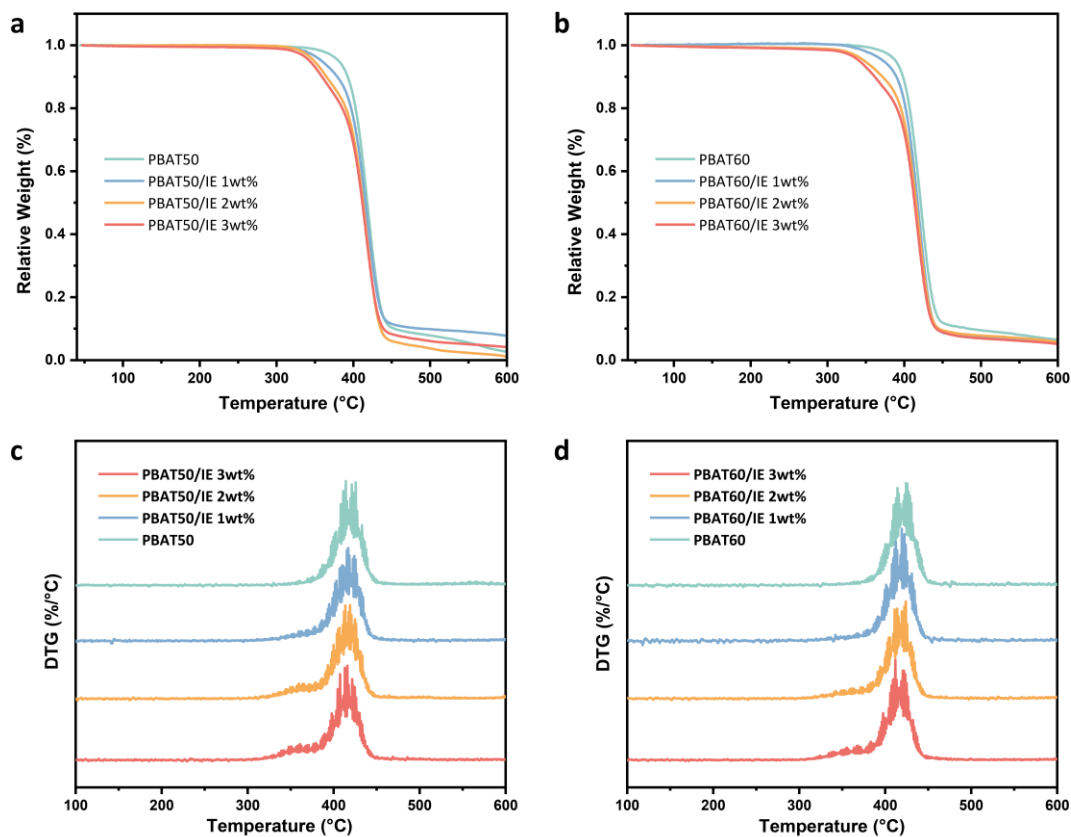


Figure S7. Thermogravimetric (a and b) and differential thermal gravimetric (c and d) curves of PBAT and PBAT/IE (1-3 wt%).

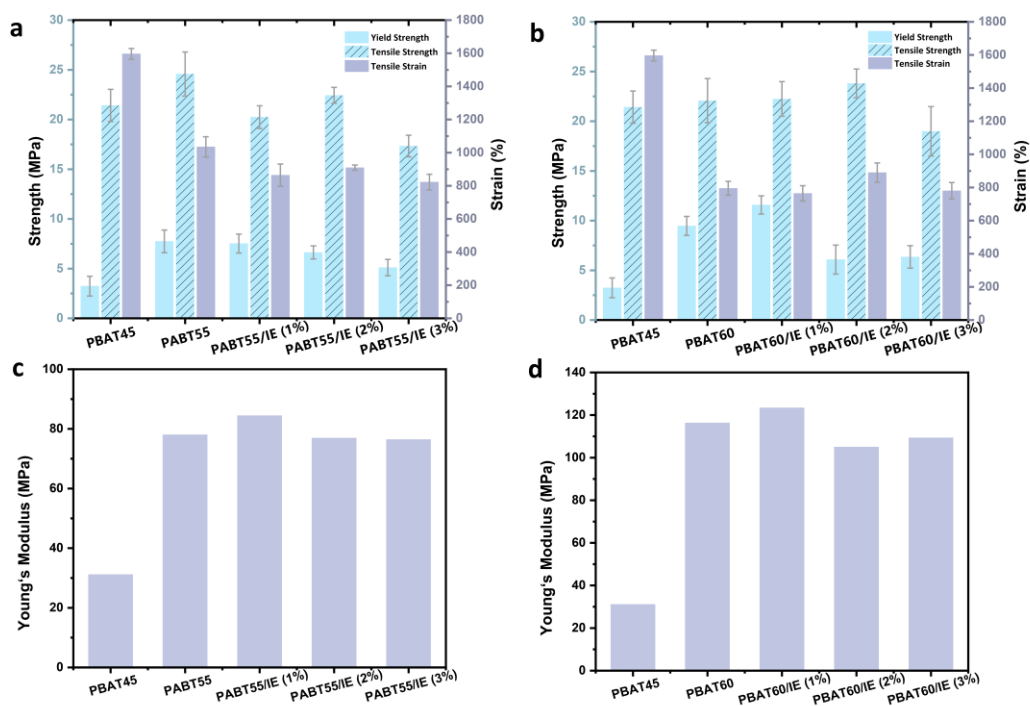


Figure S8. Tensile strength, yield strength, strain (a and b) and young's modulus (c and d) of PBAT and PBAT with immobilized enzyme.

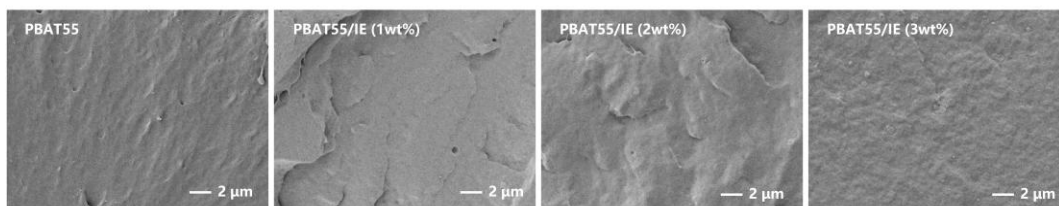


Figure S9. SEM images of nanoparticle dispersion in PBAT45 with different immobilized enzyme loadings

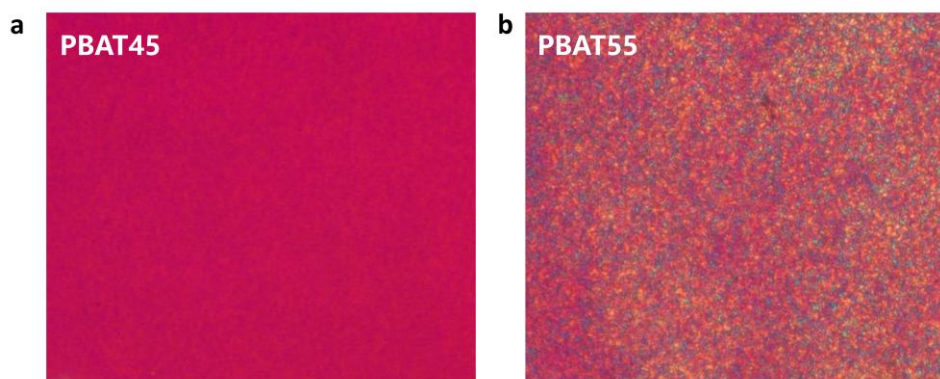


Figure S10. Polarizing microscope (POM) image of PBAT45 and PBAT55.

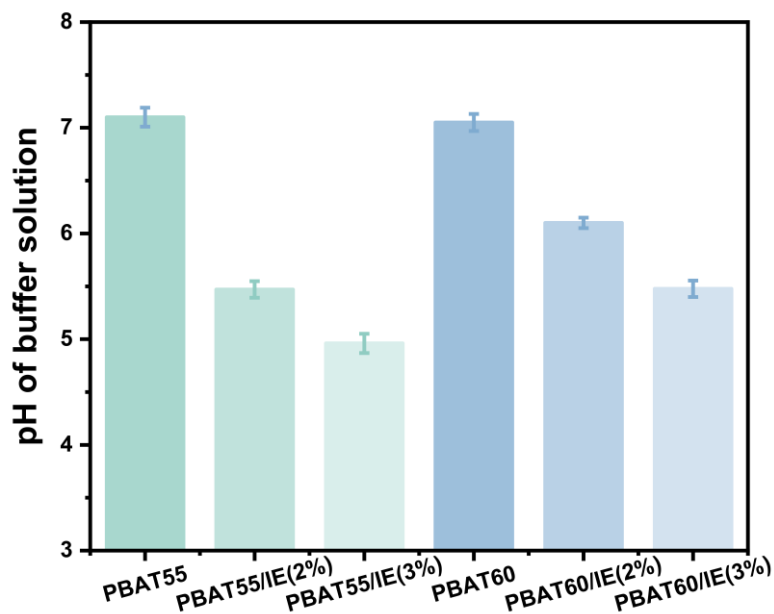


Figure S11. The pH variations of the PBS buffer solution containing PBAT and PBAT/IE composites films without intervention after 40 days' degradation.

As the degradation proceeds, the rate gradually slows down, which is attributed to the production of acidic substances (terephthalic acid, adipate acid, benzoic acid and other soluble acid) within the system (1, 2), leading to a change in pH that affects the enzyme activity, thereby resulting in a slower degradation rate, shown in **Figure S9**.

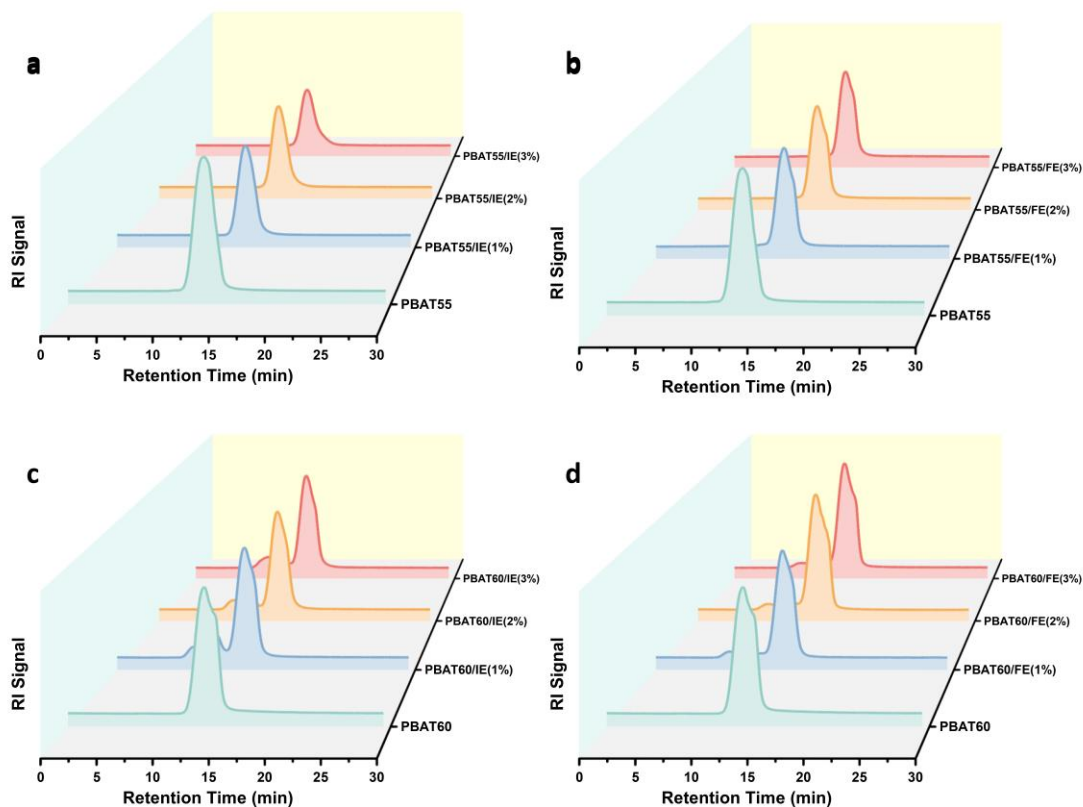


Figure S12. Gel permeation chromatography elution curve of PBAT/IE and PBAT/FE composites after 54 days' hydrolysis. (a) Immobilized enzyme embedded PBAT55 with 0-3wt% loadings. (b) Free enzyme embedded PBAT55 with 0-3wt% loadings. (c) Immobilized enzyme embedded PBAT60 with 0-3wt% loadings. (d) Free enzyme embedded PBAT60 with 0-3wt% loadings.

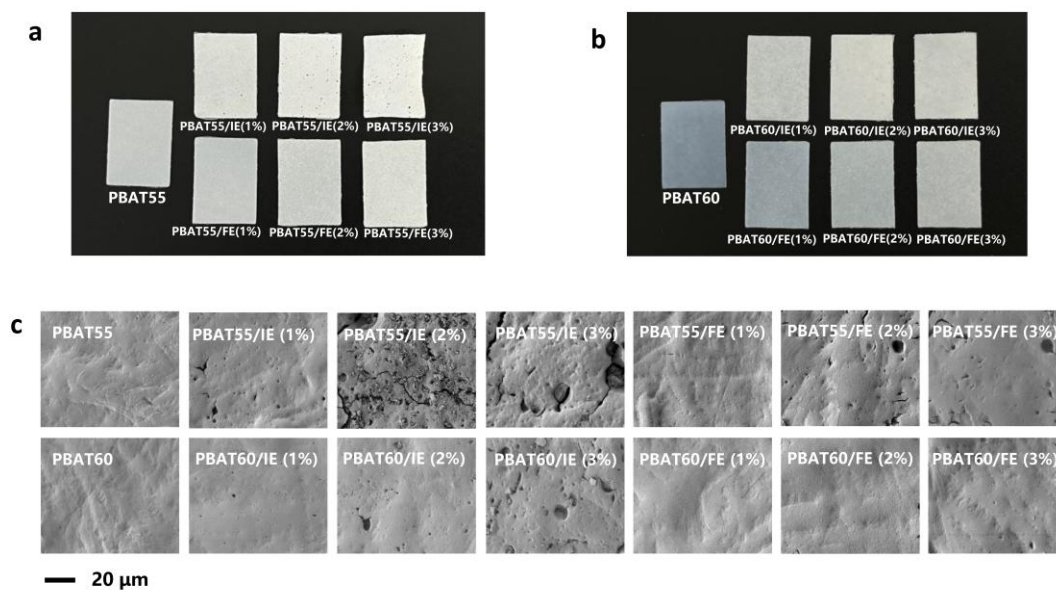


Figure S13. Digital (a and b) and SEM (c) images of PBAT55 (a) and PBAT60 (b) with immobilized enzyme (IE) or free enzyme (FE) embedding after degradation.

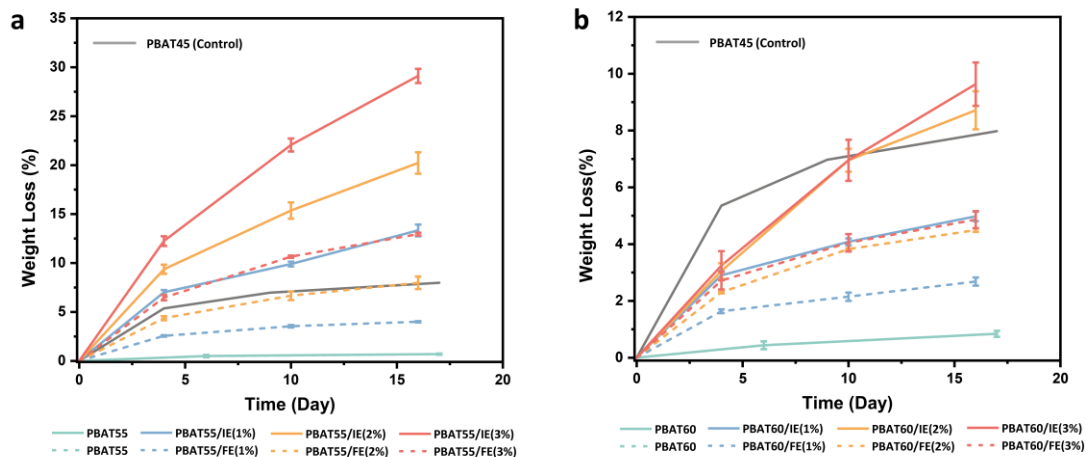


Figure S14. Weight loss curve of PBAT55 (a) and PBAT60 (b) containing 1-3 wt% immobilized and free enzyme compared with conventional PBAT45.

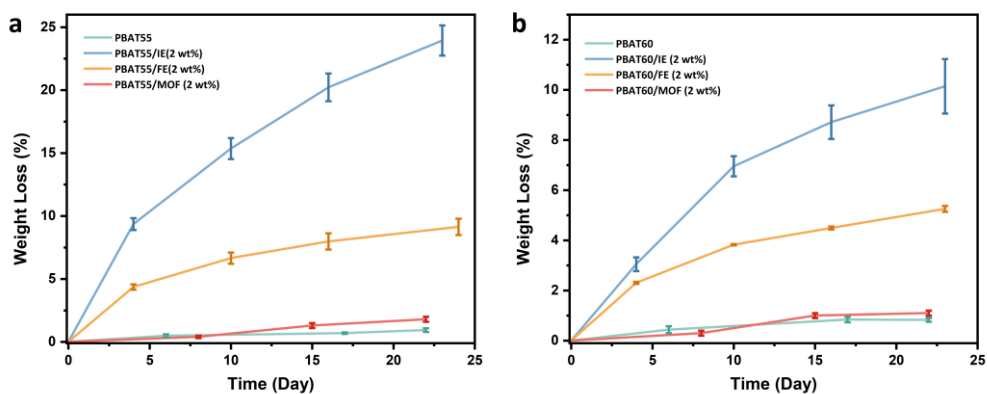


Figure S15. Weight loss curve of PBAT55 (a) and PBAT60 (b) containing 2 wt% MOF without enzyme.

References

1. Fei F, Su Z, Liu R, Gao R, Sun C. Efficient biodegradation of poly(butylene adipate-co-terephthalate) in mild temperature by cutinases derived from a marine fungus. *J Hazard Mater.* 2024;480:136008.
2. Liu T-Y, Zhen Z-C, Zang X-L, Xu P-Y, Wang G-X, Lu B, et al. Fluorescence tracing the degradation process of biodegradable PBAT: Visualization and high sensitivity. *J Hazard Mater.* 2023;454:131572.